Feasibility Study of Tumor Monitoring Technique using Prompt Gamma Rays during Antiproton Therapy

Han-Back Shin

Department of Biomedical Engineering
Research Institute of Biomedical Engineering
College of Medicine
The Catholic University of Korea

Introduction

- The antimatter was firstly proposed by P. A. M. **Dirac** in 1928 (**Nobel prize** in 1933)
  - Same mass, Opposite charge

- Antiprotons were discovered in 1955 by **Chamberlain** *et al*. (**Nobel prize** in 1959)
  - The stable antiparticle of the proton; negative charge and different magnetic moment

- In 1984, **L. Gray** *et al*. suggested **cancer therapy with antiprotons**
- **Antiproton production**; collision of protons accelerated at the velocity of light with a copper plate or iridium rod.

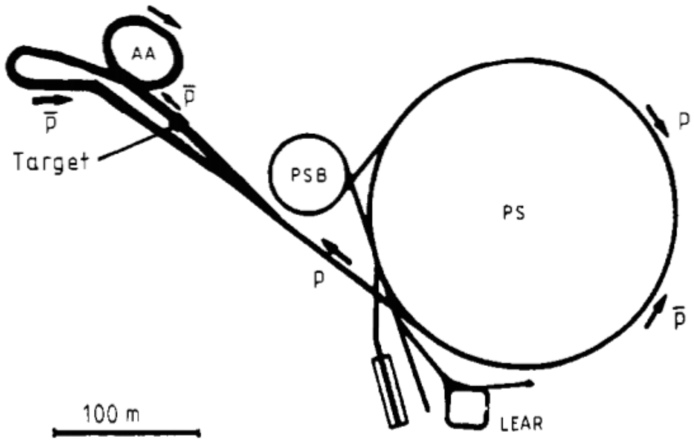

Figure 1. Layout of the accelerator complex used to produce low-energy antiprotons. Protons of 26 GeV extracted from the proton synchrotron (PS) strike a target to produce antiprotons. These are then collected in the accumulator ring (AA) before being sent back to the proton synchrotron where they are decelerated and sent to the low-energy antiproton storage ring LEAR.

A. H. Sullivan. "A measurement of the local energy deposition by antiprotons coming to rest in tissue-like material.." *Physics in medicine and biology* 30.12 (1985)

Introduction

- An antiproton almost entirely behave as protons.
  - ✓ An antiproton is an new candidate for radiation therapy.
  - ✓ Additionally the recoiling fragments contributed with an **increased relative biological efficiency (RBE) around the annihilation**

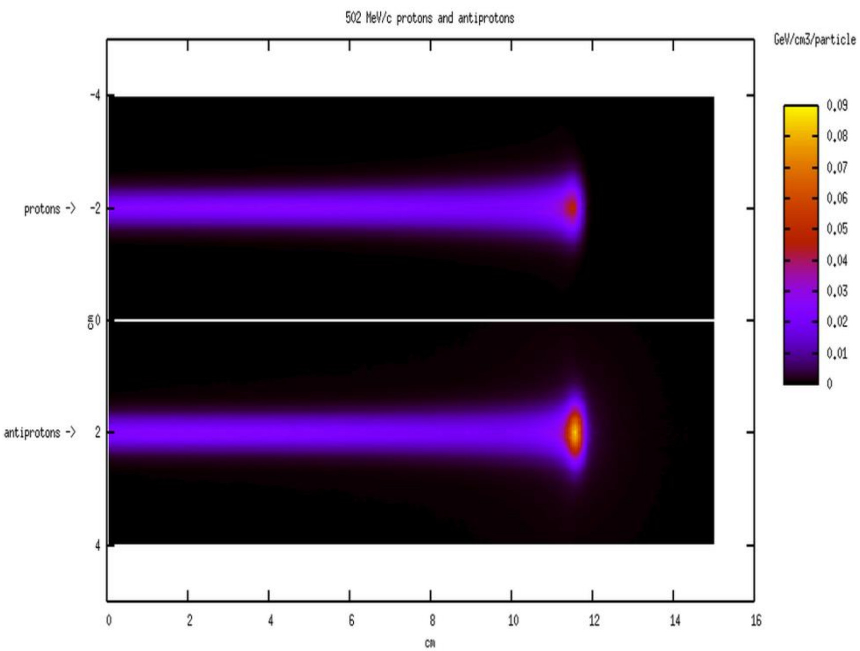

N. Bassler. “Experimental studies relevant for antiproton cancer therapy.” PhD thesis, University of arahus (2006)

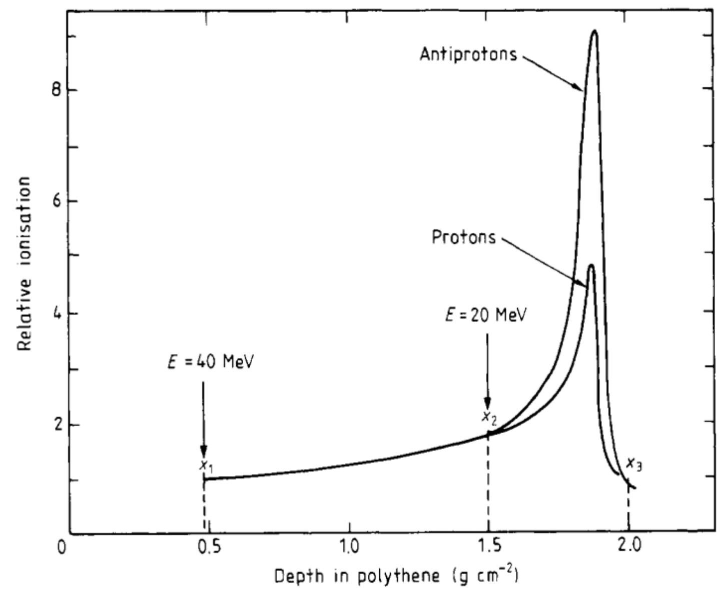

Figure 3. Variation of energy deposition by beams of protons and antiprotons with depth in an absorber. Each curve normalised to 1 at a depth of 0.5 g cm^{-2}.

A. H. Sullivan. “A measurement of the local energy deposition by antiprotons coming to rest in tissue-like material.." *Physics in medicine and biology* 30.12 (1985)

Introduction

▪ The biologically effective dose ratio of antiproton is **four times more effective** than the conventional proton for cell irradiation

▪ **Amplification of the therapeutic effect** of **proton boron fusion therapy** compared with proton therapy

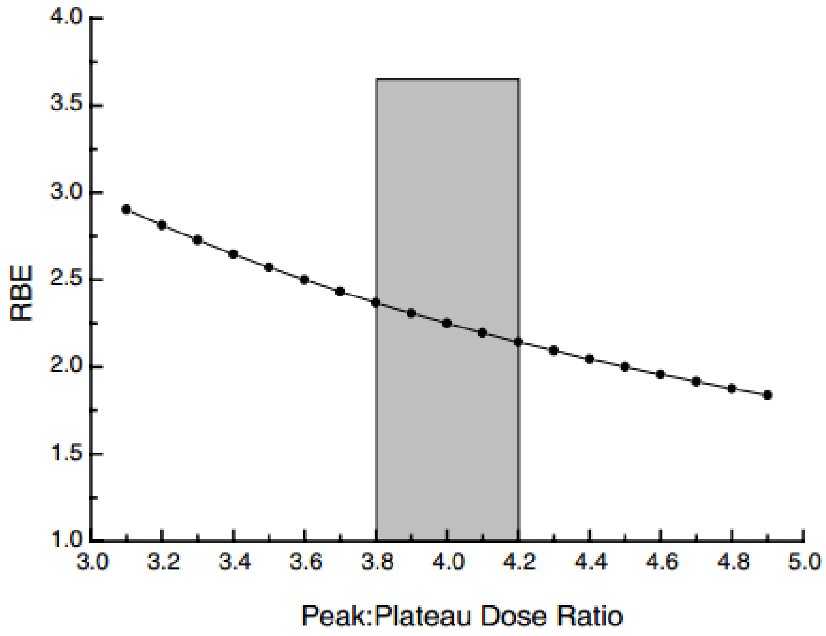

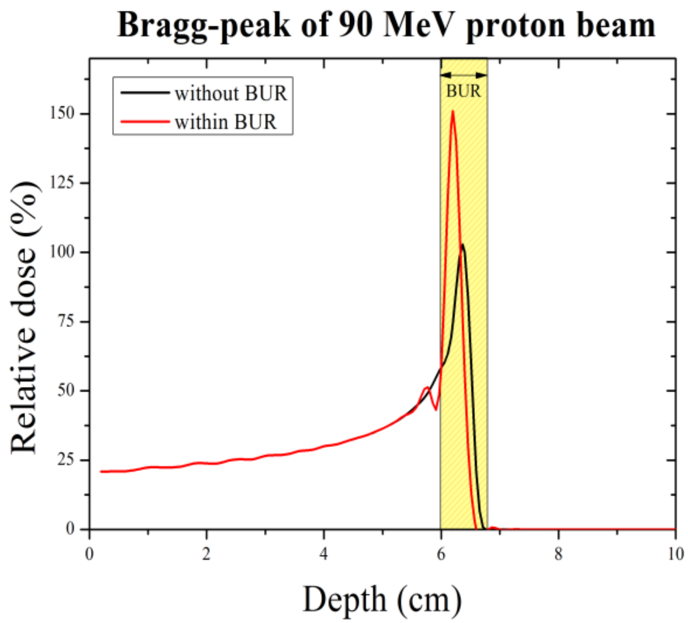

M. H. Holzscheiter., et al. "The biological effectiveness of antiproton irradiation." *Radiotherapy and oncology* 81.3 (2006)

D. K. Yoon., et al. "Application of proton boron fusion reaction to radiation therapy: A Monte Carlo simulation study." *Applied Physics Letters* 105.22 (2014)

Introduction

Schematic of ^{10}Boron Neutron Interaction

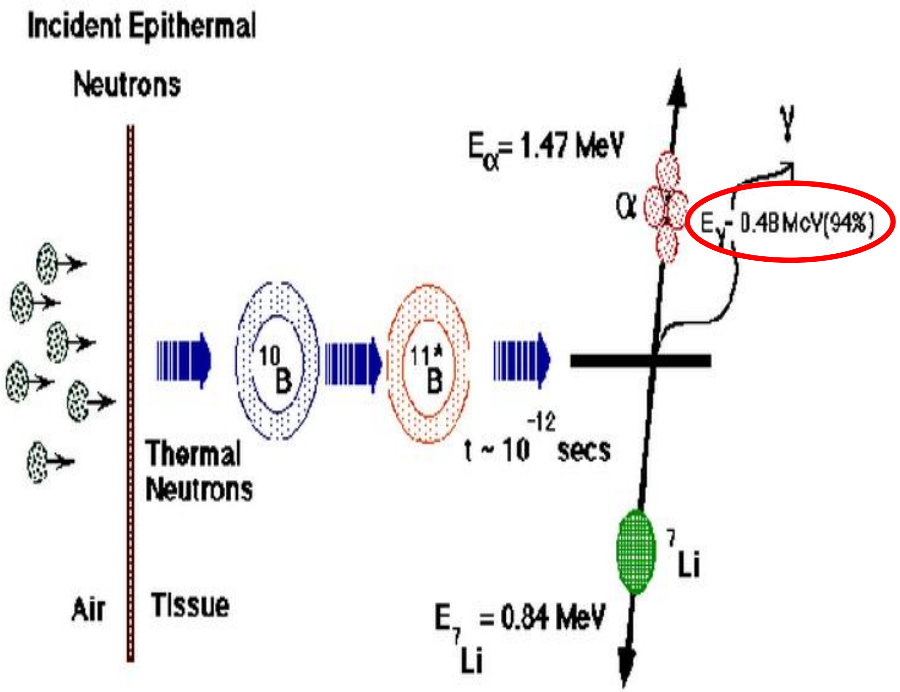

Ref. http://web.mit.edu/nrl/www/bnct/info/description/description.html

Prompt gamma ray Imaging

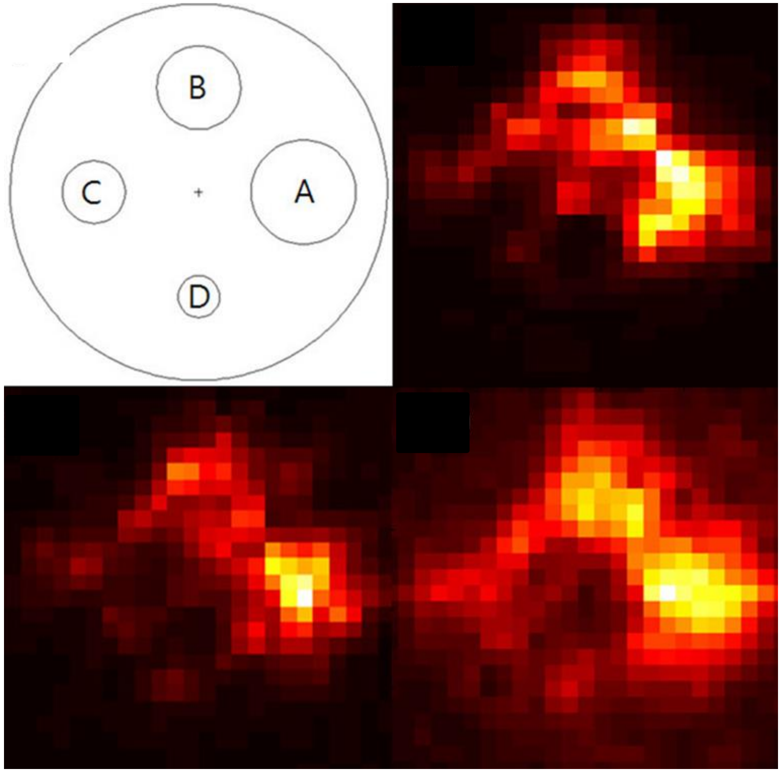

D. K. Yoon., et al. “GPU-based prompt gamma ray imaging from boron neutron capture therapy." *Medical Physics* 42.1 (2015)

Introduction

Neutron boron capture reaction

$$^{10}B + {}^{1}n \xrightarrow{\sigma_B} {}^{11}B^*$$

$$\xrightarrow{93.9\%} {}^{4}He + {}^{7}Li^* \longrightarrow {}^{7}Li + \gamma(478keV)$$

$$\xrightarrow{6.1\%} {}^{4}He + {}^{7}Li$$

$$^{1}H + {}^{1}n \xrightarrow{\sigma_H} {}^{2}H + \gamma(2223keV)$$

FIG. 1. Simplified decay chains following neutron capture reactions in boron and hydrogen. The neutrons captured are mainly of thermal energy (~0.025 eV) as the capture cross sections (σ_B and σ_H, respectively) are the highest at that energy. An asterisk indicates that the nucleus is in an excited state. The disintegration of the excited boron-11 nucleus follows two branches.

P. M. M. af Rosenschold., et al. "Toward clinical application of prompt gamma spectroscopy for in vivo monitoring of boron uptake in boron neutron capture therapy." *Medical Physics* 28. 5. (2001)

Proton boron fusion reaction

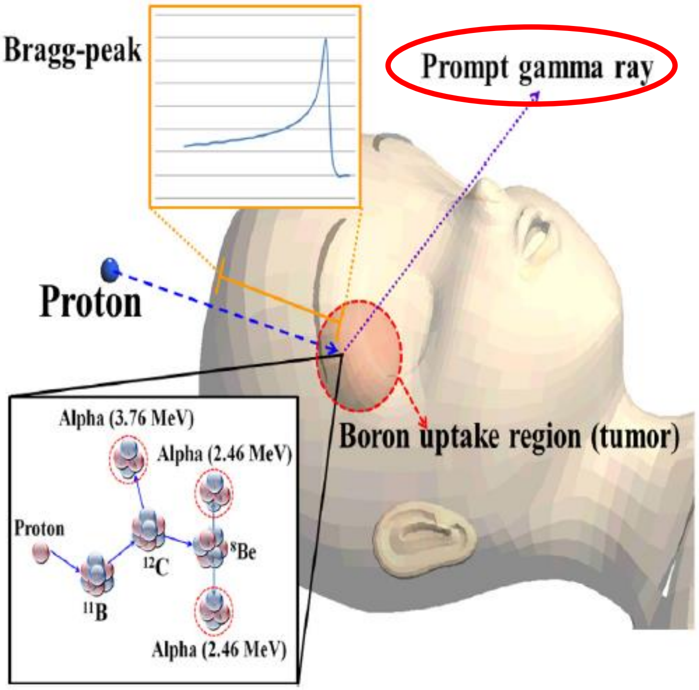

D. K. Yoon., et al. "Application of proton boron fusion reaction to radiation therapy: A Monte Carlo simulation study." *Applied Physics Letters* 105.22 (2014)

Purpose

Verification of **the therapeutic effect** of the antiproton boron fusion therapy and **the acquisition of the tomographic image** using prompt gamma ray

Materials and Methods

❖ Simulation set-up

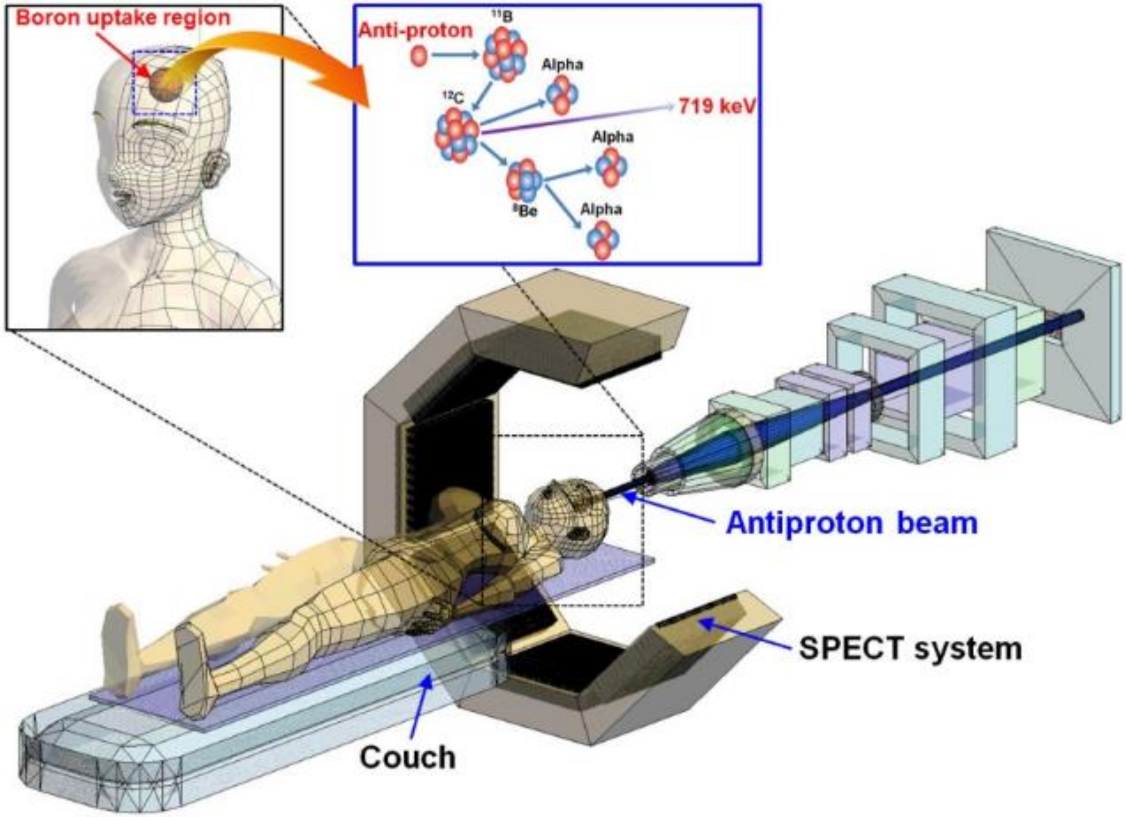

- Monte Carlo n-particle simulation (MCNPX 2.6.0, LANL)
- Parallel collimator, Three boron uptake regions
- Prompt gamma-ray is emitted from reaction point (719 keV)

Materials and Methods

◆ System specification

- Water phantom
  - Density= 1 g/cm^3, diameter: 160 mm, height: 100 mm
- Three boron uptake regions
  - A (15.0, -13.2), B(-18.9, -6.4), C(3.9, 19.6)
  - Height: 20 mm
  - Boron concentration: 780 μg/g
- Detector
  - LYSO (density= 7.3 g/cm^3)
  - Tungsten parallel collimator (density= 17.3 g/cm^3)
    - Height: 8 cm, thickness: 2.5 mm

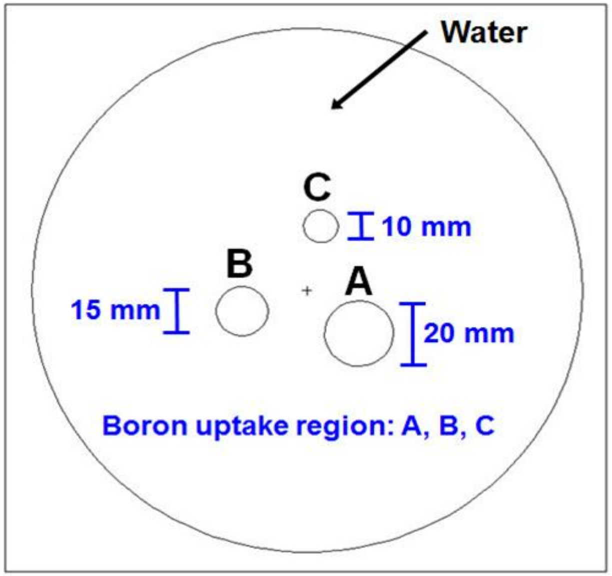

◆ Percentage depth dose

➢ F6 tally (absorbed dose) in MCNPX

◆ Energy spectrum

➢ F8 tally (energy deposition) in MCNPX

◆ Image reconstruction using prompt gamma ray

➢ A 80 × 80 pixel matrix with a pixel size of 5 mm

◆ Image profile & receiver operating characteristic (ROC)

➢ Tolerance value: 10%

Results and Discussion

❖ Percentage depth dose

❖ Energy spectrum

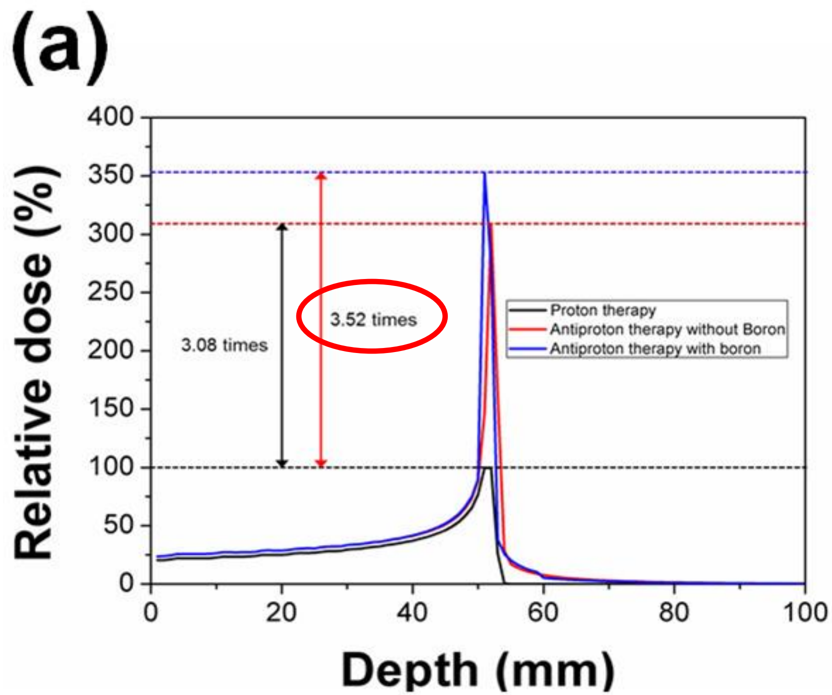

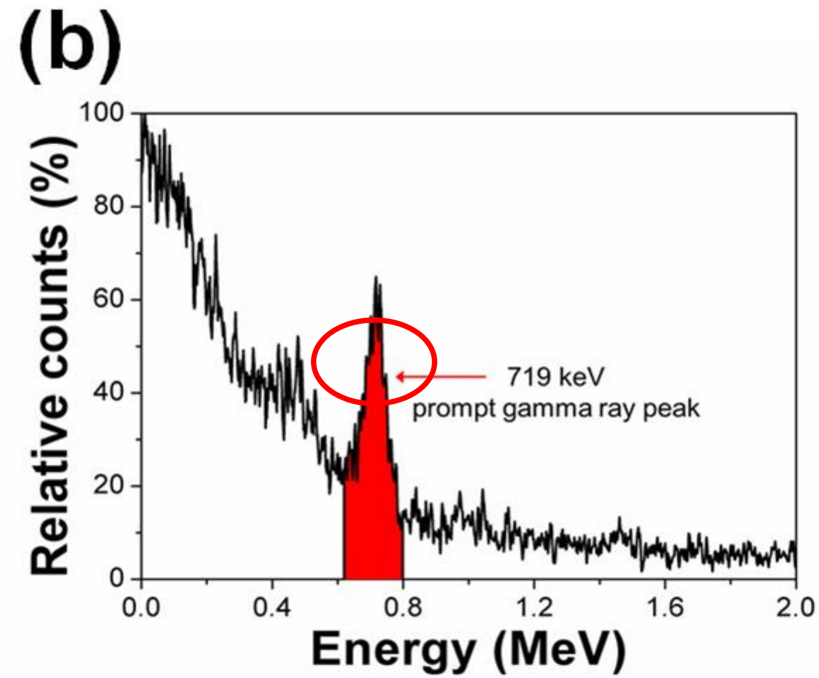

(a) Percentage depth dose (PDD) of proton and antiproton beams from the water phantom with and without BURs. (b) Energy spectrum of prompt gamma ray from the reaction between an antiproton and boron.

- The maximum value of antiproton with/without boron is **three times greater than** that of conventional proton PDD line.
- **The prompt gamma ray peak at 719 keV** can be clearly **observed** in the spectrum.

Results and Discussion

❖ Reconstructed image

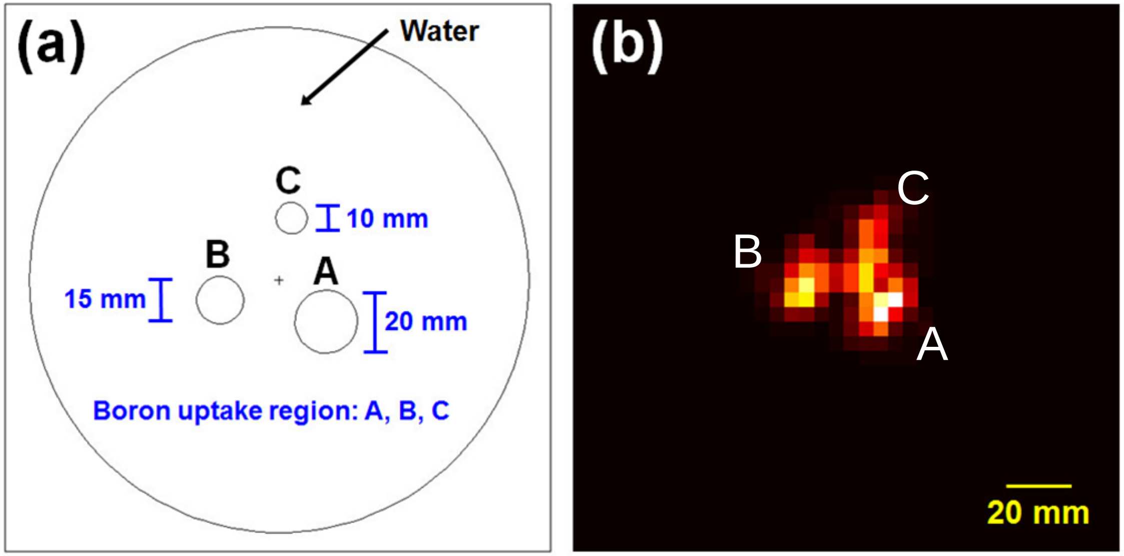

(a) Original pattern of the water phantom including the three boron uptake regions (BURs).
(b) Reconstructed image using the prompt gamma ray events.

- Energy window: 10%
- MLEM reconstruction algorithm using 32 projections
- The values of the signal-to-noise ratio: 13.26 (A), 12.82 (B), 8.31 (C)

Results and Discussion

❖ Image profile ❖ ROC curve

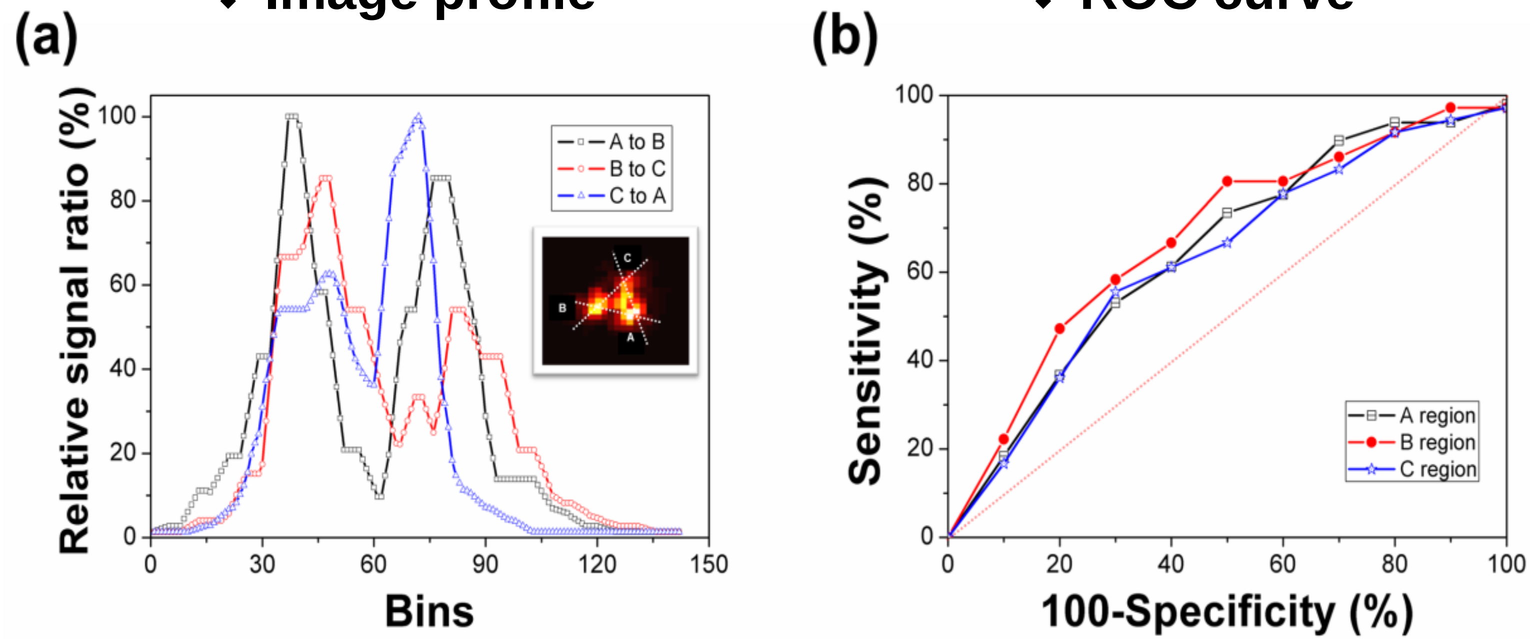

(a) Image profiles of three lines on the reconstructed image. (b) ROC curve regarding the three boron uptake regions

- Estimation of the size of the BURs: 15-20 mm (A), 10-15 mm (B), 10 mm (C)
- The area under the curve (AUC): 0.647 (A), 0.679 (B), 0.632 (C)
  - ✓ 0.6-0.7: **acceptable**

Conclusion

- ✓ **Amplification of the therapeutic effect** of the antiproton boron fusion therapy compared with antiproton and proton

- ✓ Possibility of the **tumor monitoring** using prompt gamma ray
  - ➢ A promising and useful technique as real-time monitoring
  - ➢ Provide guidance for a more accurate radiation therapy

- ✓ In future work
  - ➢ Further simulation including a clinical factor
  - ➢ Optimization of reconstruction parameters

Thanks for your attention!

Han-Back Shin

hbshin07@catholic.ac.kr

Department of Biomedical Engineering
Research Institute of Biomedical Engineering
College of Medicine
The Catholic University of Korea